Predictive event-triggered control for string-stable platooning

Etienne Gorski, Irinel-Constantin Morârescu, Vineeth Satheeskumar Varma, Lucian Buşoniu

Predictive event-triggered control for string-stable platooning ⋆

Etienne Gorski [*,**] **Irinel-Constantin Morărescu** [*,**]
Vineeth Satheeskumar Varma [*,**] **Lucian Buşoniu** [**,***]

[*] *Université de Lorraine, CNRS, CRAN, F-54000 Nancy, France*
[**] *Automation Department, Technical University of Cluj-Napoca, 400114 Cluj-Napoca, Romania*
[***] *Corresponding Member of the Romanian Academy, Bucharest, Romania*

Abstract: This paper presents an event-triggered control strategy for vehicle platoons that use Cooperative Adaptive Cruise Control (CACC). In contrast to classical CACC, which relies on continuous communication of each vehicle's control input to its next follower, we propose a framework in which each vehicle intermittently communicates a longer-horizon prediction of its control trajectory. A non-standard, predictive flavor of event-triggered control (ETC) results, in which these more informative predictions are used instead of the usual zero- or first-order-hold signal reconstruction. Communications are triggered by usual ETC rules, when the error between the real input trajectory and the predicted one exceeds a design threshold. By exploiting model-based predictions, we achieve a significantly reduced number of communications, while guaranteeing individual and string stability through a Lyapunov-based analysis. Numerical simulations with instantaneous and sustained perturbations on a seven-vehicle platoon illustrate the effectiveness of the proposed framework.

Keywords: Platooning, Event-triggered control, Prediction-based control, String stability

1. INTRODUCTION

The increasing prevalence of connected and automated vehicles (CAVs) allows improving traffic efficiency, road safety, and energy consumption. Among the most promising strategies is vehicle platooning, where a group of vehicles travel in a tight formation with coordinated acceleration and braking. Platooning not only reduces inter-vehicle spacing, increasing road throughput, but also minimizes aerodynamic drag, leading to substantial fuel savings (Shladover, 2018). However, the safe and efficient operation of platoons critically depends on accurate coordination among vehicles, which is inherently linked to both control design and inter-vehicle communication.

Cooperative Adaptive Cruise Control (CACC) became a standard strategy for platooning. In addition to onboard sensors, CACC uses a communication network to share control information across multiple vehicles in the platoon (Swaroop, 1997; Ploeg et al., 2013). This cooperative aspect allows each vehicle to anticipate the actions of its predecessors, improving string stability, damping propagation of disturbances, and enabling smaller inter-vehicle gaps. Crucially, this cooperation relies on a communication network, typically based on Vehicle-to-Vehicle (V2V) links (Giambene et al., 2020), although other architectures such as cellular vehicle-to-everything or hybrid schemes are also possible (Trabelsi et al., 2024). Continuous exchange of control signals ensures quiet responses, but can overwhelm network bandwidth and increase latency, particularly in large platoons or congested traffic scenarios (Nardini et al., 2018).

To address these challenges, Event-Triggered Control (ETC) has emerged. Unlike traditional time-triggered control, where information is transmitted periodically, ETC only sends updates when a certain event or condition is violated, reducing network load while preserving stability (Tabuada, 2007). The use of ETC in CACC allows more feasible usage of the communication network within the platoon. In this context, we focus on the problem of reducing communication in vehicle-to-vehicle-controlled vehicle platoons under CACC while ensuring both individual and string stability.

Unlike standard ETC results, we propose a strategy based on the communication of predicted control inputs for platooning. Each vehicle predicts its future input using a nominal model of its internal dynamics. This predicted input is then transmitted, and the follower receives updates only when the actual signal significantly deviates from the predicted one. This approach offers several advantages:

- a reduction in communication load, as transmissions occur only when deviations from the model are observed (Jang and Kim, 2024);
- improved transient tracking due to the reconstruction of a continuous and dynamically consistent signal (Razzaghpour et al., 2023);

⋆ This work was been financially supported from the project DECIDE, no. 57/14.11.2022, funded under the PNRR I8 scheme by the Romanian Ministry of Research, Innovation and Digitisation and also partially funded by ANR under the grant COMMITS No. ANR-23-CE25-0005.

- compatibility with individual and string stability guaranties obtained via LMI-based Lyapunov methods.

To the best of our knowledge, this approach introduces several novelties compared to the existing literature on CACC. It combines internal vehicle modeling and dynamic prediction of the control signal with event-triggered communication, while most previous works rely on Zero- or First-Order-Hold reconstruction (He et al., 2018) or, more recently, reinforcement learning methods (Dang et al., 2024). While predictive ETC has been used in networked control systems (Varutti et al., 2009) where only individual system stability is of interest, it has not been implemented and theoretically analyzed for platooning, where the main difficulty is string stability. Our method provides a theoretical framework to ensure individual and string stability in the presence of disturbances and limited transmissions, while ensuring a practical implementation that avoids Zeno phenomena. Note that while the number of transmissions is expected to decrease significantly, each communication packet with the predicted trajectory will be larger than the classical packet that contains only the current control input. However, in the IEEE 802.11p standard for vehicle-to-vehicle communications, packets of up to 500 bytes are allowed, which by using efficient compression allows interesting predicted signals to be communicated, while reducing packet collisions due to the fewer transmissions (Toker et al., 2018).

The paper is organized as follows Section 2 describes the platoon model used. Section 3 presents the stability analysis for coupled systems under ETC, as well as the conditions for both stabilities. Section 4 details the construction of the predicted signal. Section 5 illustrates the performance of the proposed method through numerical simulations on a vehicle platoon subject to different scenarios. Finally, Section 6 summarizes the contributions and suggests directions for future work.

2. FRAMEWORK

2.1 Setup and Dynamics

We consider a platoon composed of N homogeneous vehicles indexed by $i \in \{1, \dots, N\}$, which follow a leading vehicle indexed by $i = 0$. The goal of each vehicle i is to follow its predecessor $i-1$ while maintaining a safe inter-vehicle distance defined by a constant time-gap policy. More precisely, the desired inter-distance at time $t \in \mathbb{R}^+$ is given by

$$d_{r,i}(t) = r + hv_i(t), \tag{1}$$

where r is the minimum safety margin, $h > 0$ the desired time-gap, and $v_i(t)$ the velocity of vehicle i at time t.

The vehicle spacing error i is defined as

$$e_i(t) = q_{i-1}(t) - q_i(t) - hv_i(t) - r - L, \tag{2}$$

where $q_i(t)$ denotes the position of vehicle i and L is the common vehicle length. Each vehicle is modeled as a third-order dynamical system with input filtering, according to Dolk et al. (2017). Specifically, the longitudinal dynamics of vehicle $i \geq 1$ are described by

$$\dot{e}_i(t) = v_{i-1}(t) - v_i(t) - ha_i(t), \tag{3a}$$

$$\nu_i : \begin{cases} \dot{v}_i(t) = a_i(t), \\ \dot{a}_i(t) = -\dfrac{1}{\tau}a_i(t) + \dfrac{1}{\tau}u_i(t), \end{cases} \tag{3b}$$

$$\dot{u}_i(t) = -\frac{1}{h}u_i(t) + \frac{1}{h}\chi_i(t), \tag{3c}$$

where $a_i(t)$ is the acceleration, $u_i(t)$ the desired acceleration, $\chi_i(t)$ the control input, and $\tau > 0$ the inertia constant, common for all vehicles.

Equation (3a) follows directly by differentiating (2). The filter dynamics (3c) implement a pre-compensation of the time-gap policy with transfer function $H(s) = hs + 1$, whose inverse cancels the delay induced by h in the control loop . This choice decouples closed-loop stability from the specific value of h, providing design flexibility (Ploeg et al., 2013).

The leading vehicle $i = 0$ is described by

$$\nu_0 : \begin{cases} \dot{v}_0(t) = a_0(t), \\ \dot{a}_0(t) = -\dfrac{1}{\tau}a_0(t) + \dfrac{1}{\tau}u_0(t), \end{cases} \tag{4}$$

with $u_0(t)$ being an exogenous input. The first follower error $e_1(t)$ therefore captures the deviation of vehicle 1 from its reference distance with respect to the leader.

2.2 Control Input and Stability Requirements

We briefly recall that in the CACC scheme, the control input $\chi_i(t)$ of vehicle i combines two contributions: (i) a feedback term based on local sensors that provide vehicle speed and acceleration measurements, and (ii) a feedforward term based on the predecessor's desired acceleration $u_{i-1}(t)$. Formally, we write:

$$\chi_i(t) = k_p e_i(t) + k_d \dot{e}_i(t) + \hat{u}_{i-1}(t), \tag{5}$$

where $k_p, k_d > 0$ are controller gains and $\hat{u}_{i-1}(t)$ denotes the estimate of the predecessor's demanded acceleration. The latter is transmitted via a communication network from the previous vehicle.

The platoon must satisfy two key stability properties:

- **Individual stability:** in the absence of input from the predecessor ($\chi_{i-1}(t) = 0$), each vehicle's spacing error $e_i(t)$ must converge asymptotically to zero. This property ensures that, if the leader maintains a constant velocity, all following vehicles will asymptotically reach their desired equilibrium velocities.
- **String stability:** when the leader is subject to a bounded change in the input $u_0(t)$ (due e.g. to unforeseen incidents on the road), the resulting perturbations must not amplify along the vehicle string. From Feng et al. (2019), this can be expressed as an $\mathcal{L}_2$-gain condition between consecutive control signals
$$\|\chi_i\|_{L_2} \leq \gamma \|\chi_{i-1}\|_{L_2}, \quad \text{with } \gamma < 1, \ \forall i \geq 1.$$
This property ensures that velocity fluctuations are attenuated throughout the platoon, thereby preventing oscillations (i.e. phantom traffic jams), collisions, or large spacing errors.

2.3 Event-Triggered Communication

In conventional control systems, information between subsystems or agents is typically exchanged at fixed sampling

intervals, leading to periodic communication regardless of the system state. In contrast, event-triggered communication transmits information based on the system state or the control error. In vehicle platoons, it allows a vehicle to send its control signals to followers only when needed, i.e. when a certain threshold on the error signal $e_{u,i-1} = \hat{u}_{i-1} - u_{i-1}$ is exceeded, ensuring safe spacing and efficient communication.

Two cases of triggering rule will be addressed in the theoretical analysis of Section 3. First, we study a proportional triggering condition of the form

$$\|e_{u,i-1}(t)\| \leq \sigma \|x_i(t)\|, \tag{6}$$

where $\sigma > 0$ is chosen to guarantee stability and string stability via Theorem 1.

Then, a constant-threshold triggering rule is studied via Theorem 2:

$$\|e_{u,i-1}(t)\| \leq \varepsilon, \tag{7}$$

where $\varepsilon > 0$ is a small positive constant. This modification prevents asymptotic stability but reduces communications due to very small state norms (avoiding a Zeno-like behavior) while still ensuring good system performance. The parameter ε thus introduces a practical margin, allowing the system to operate efficiently under realistic network constraints.

Other event-triggering strategies can also be considered. For instance, a mixed threshold $\|e_{u,i-1}(t)\| \leq \max(\varepsilon, \sigma\|x_i(t)\|)$ combines a constant bound with a state-dependent term, reducing communication when the state is small while preserving performance for larger deviations. More sophisticated dynamic triggering laws can adapt the threshold online based on system states, error evolution, or network conditions, potentially improving the trade-off between communication load and control accuracy. The purpose of this paper is to present and validate the concept of predictive ETC, therefore only proportional and constant trigger rules will be discussed. Further research is needed to adapt other rules.

Our method departs from classical ZOH ETC approaches, where the transmitted signal is typically held constant between two transmission instants (i.e., $\dot{\hat{u}}_{i-1}(t) = 0$ for $t \in [t_k, t_{k+1})$). At each triggering instant t_k, we transmit not only the current value $u_{i-1}(t_k)$, but also additional information that allows vehicle i to reconstruct the anticipated evolution of its predecessor's control input. Specifically, the signal $\hat{u}_{i-1}(t)$ evolves according to

$$\dot{\hat{u}}_{i-1}(t) = f_{i-1}(t - t_k), \quad t \in [t_k, t_{k+1}), \tag{8}$$

where f_{i-1} is a prediction function of vehicle $i-1$. Its construction is detailed in Section 4 of this paper.

This time-varying reconstruction is the key novel aspect of our approach. Compared to standard ZOH-based ETC, it provides two main advantages:

- It reduces the mismatch between $u_{i-1}(t)$ and $\hat{u}_{i-1}(t)$, improving control performance even with sparse transmissions.
- It can compensate for network imperfections such as delays, sampling effects, and noise, since the transmitted prediction aligns with the expected value at the time of reception rather than the time of transmission. However, this aspect will not be addressed in this paper.

This new ETC perspective requires revisiting both the *individual stability* and the *string stability* requirements, since the additional dynamics of $\hat{u}_{i-1}$ must now be included in the closed-loop system; we perform this latter step next, followed by stability analysis in Section 3.

2.4 State-space Representation

For analysis purposes, it is convenient to rewrite the differential equations (3)–(5) in a state-space form. To this end, the state vector for vehicle i's model must capture the dynamics of both vehicles i and $i-1$.

Specifically, for each follower $i \geq 1$, we define the state as

$$x_i(t) := \begin{bmatrix} v_{i-1}(t) - v_i(t) \\ a_{i-1}(t) \\ u_{i-1}(t) \\ e_i(t) \\ a_i(t) \\ u_i(t) \end{bmatrix} \in \mathbb{R}^6. \tag{9}$$

The components of $x_i(t)$ include: (i) the relative velocity between vehicle $i-1$ and i, (ii)–(iii) the acceleration and demanded acceleration of the predecessor $i-1$, (iv) the spacing error of vehicle i, (v)–(vi) the acceleration and demanded acceleration of vehicle i.

With this construction, the closed-loop dynamics for vehicle i can be expressed as

$$\begin{cases} \dot{x}_i(t) = Ax_i(t) + B\chi_{i-1}(t) + Ee_{u,i-1}(t) \\ \dot{e}_{u,i-1}(t) = Bx_i(t) - \frac{1}{h}\chi_{i-1}(t) + f_{i-1}(t - t_k), \\ \chi_i(t) = Cx_i(t) + e_{u,i-1}(t) \end{cases} \tag{10}$$

with

$$A = \begin{bmatrix} 0 & 1 & 0 & 0 & -1 & 0 \\ 0 & -\frac{1}{\tau} & \frac{1}{\tau} & 0 & 0 & 0 \\ 0 & 0 & -\frac{1}{h} & 0 & 0 & 0 \\ 1 & 0 & 0 & 0 & -h & 0 \\ 0 & 0 & 0 & 0 & -\frac{1}{\tau} & \frac{1}{\tau} \\ \frac{k_d}{h} & 0 & \frac{1}{h} & \frac{k_p}{h} & -k_d & -\frac{1}{h} \end{bmatrix}, \quad B = \begin{bmatrix} 0 & 0 & \frac{1}{h} & 0 & 0 & 0 \end{bmatrix}^\top,$$

$$C = [k_d \ 0 \ 1 \ k_p \ -hk_d \ 0], \quad E = \begin{bmatrix} 0 & 0 & 0 & 0 & 0 & \frac{1}{h} \end{bmatrix}^\top.$$

It is important to note that, in this formulation, $e_{u,i-1}$ evolves under the exogenous excitation f_{i-1}. As a result, $\dot{e}_{u,i-1}$ cannot be expressed as a linear combination of state components in x_i. In the absence of the exogenous term (i.e., under the classical ZOH assumption where $\dot{\hat{u}}_{i-1} = 0$), the signal $e_{u,i-1}$ could be incorporated directly into the state vector, leading to a standard formulation

$$\begin{cases} \dot{x}_i^\star(t) = A^\star x_i^\star(t) + B^\star \chi_{i-1}(t) \\ \chi_i(t) = C^\star x_i^\star(t) \end{cases} \tag{11}$$

where $x_i^\star = (x_i, e_{u,i-1})^\top \in \mathbb{R}^7$ and $A^\star \in \mathbb{R}^{7\times 7}$, $B^\star \in \mathbb{R}^{7\times 1}$, $C^\star \in \mathbb{R}^{1\times 7}$ are the state, input and output matrices of the augmented version of system (10).

For such linear time-invariant systems, both individual stability and string stability have been studied in the literature. Individual asymptotic stability can be verified by ensuring that the state matrix is Hurwitz—either via eigenvalue analysis or by finding a positive definite matrix P such that $A^{\star\top}P+PA^{\star} \prec 0$. String stability, in turn, can be certified through H_∞ or small-gain arguments, typically expressed as an LMI condition. For example, according to Dolk et al. (2017), string stability holds if there exists $P \succ 0$ such that

$$\begin{bmatrix} A^{\star\top}P + PA^{\star} + C^{\star\top}C^{\star} & PB^{\star} \\ (PB^{\star})^{\top} & -\gamma^2 I \end{bmatrix} \prec 0. \tag{12}$$

In addition to this Lyapunov-based formulation, frequency-domain approaches have been proposed to analyze string stability in vehicle platoons. These methods rely on transfer function representations of the inter-vehicle dynamics and evaluate conditions on the magnitude of the spacing error transfer ratio, such as $|E_i(j\omega)/E_{i-1}(j\omega)| \leq 1$ for all frequencies (Chuang et al., 2013). Other approaches include passivity-based and input–output stability analysis, which offer complementary perspectives on robustness and performance (Wang and Gu, 2025).

However, in our model (10) with input prediction as in (8), due to the time-varying reconstruction introduced by f_{i-1}, a tailored stability analysis is required to capture the coupled effect between the predicted input and the vehicle dynamics. We provide such an analysis, in the following section for proportional and constant triggering rules.

3. STABILITY ANALYSIS

Before analyzing the effect of event-triggered communication and inter-vehicle coupling on individual and string stability, we must verify the individual stability of the autonomous subsystem

$$\dot{x}_i = Ax_i,$$

which corresponds to the internal closed-loop dynamics of coupled vehicles in the absence of external inputs $\chi_{i-1} = 0$ and communication errors $e_{u,i-1} = 0$. The matrix A contains the internal interactions between spacing error, velocity, acceleration, and filtered control states. As previously stated, proving that A is Hurwitz guarantees that the local feedback design provides asymptotic stability of the origin for the system. Conditions on the controller's gains k_p and k_d ensure this. In practice, it is sufficient to have $k_d > \tau k_p$ (Ploeg et al., 2014).

3.1 Stability analysis under proportional ETC

We first study system (10) under the proportional triggering rule (6). The following theorem establishes the individual and string stability under ETC, after which we provide a design procedure.

Theorem 1. (Individual and string stability under proportional predictive ETC). For system (10), assume that there exist $P = P^{\top} \succ 0$, $\gamma > 0$, $\eta > 0$, and $\sigma > 0$ such that the following LMI holds:

$$\begin{bmatrix} A^{\top}P + PA + C^{\top}C + \left(1+\frac{1}{\eta}\right)\sigma^2 I & PE + C^{\top} & PB \\ (PE + C^{\top})^{\top} & -\frac{1}{\eta}I & 0 \\ (PB)^{\top} & 0 & -\gamma^2 I \end{bmatrix} \prec 0. \tag{13}$$

Then, under the triggering rule $\|e_{u,i-1}(t)\| \leq \sigma\|x_i(t)\|$, the following properties hold:

(1) (**Individual stability**) If $\chi_{i-1} \equiv 0$, the origin $x = 0$ is globally asymptotically stable.
(2) (**String stability**) For nonzero χ_{i-1}, the system is $\mathcal{L}_2$ string stable with gain γ, i.e.

$$\|\chi_i\|_{L_2} \leq \gamma\|\chi_{i-1}\|_{L_2}. \tag{14}$$

Proof: The time derivative of $V(x_i) = x_i^{\top}Px_i$ along the trajectories of the system is

$$\dot{V} = x_i^{\top}(A^{\top}P + PA)x_i + 2x_i^{\top}PB\chi_{i-1} + 2x_i^{\top}PEe_{u,i-1}.$$

Applying Young's inequality to the cross term involving χ_{i-1} yields

$$2x_i^{\top}PB\chi_{i-1} \leq \tfrac{1}{\gamma^2}x_i^{\top}PBB^{\top}Px_i + \gamma^2\chi_{i-1}^{\top}\chi_{i-1}.$$

Next, we establish a relation between the cross term with $e_{u,i-1}$ and the square of $\chi_i = Cx_i + e_{u,i-1}$, which will help us later. We seek to ensure that

$$x_i^{\top}(A^{\top}P + PA + \tfrac{1}{\gamma^2}PBB^{\top}P)x_i + 2x_i^{\top}PEe_{u,i-1} + \chi_i^{\top}\chi_i < 0$$

which is equivalent to

$$x_i^{\top}(A^{\top}P + PA + C^{\top}C + \tfrac{1}{\gamma^2}PBB^{\top}P)x_i + 2x_i^{\top}(PE + C^{\top})e_{u,i-1} + e_{u,i-1}^{\top}e_{u,i-1} < 0.$$

Using Young's inequality with parameter $\eta > 0$ gives

$$2x_i^{\top}(PE + C^{\top})e_{u,i-1} \leq \eta\, x_i^{\top}(PE + C^{\top})(PE + C^{\top})^{\top}x_i + \tfrac{1}{\eta}e_{u,i-1}^{\top}e_{u,i-1}.$$

Under the triggering condition $\|e_{u,i-1}\| \leq \sigma\|x_i\|$, one obtains

$$x_i^{\top}\Big(A^{\top}P + PA + C^{\top}C + \tfrac{1}{\gamma^2}PBB^{\top}P + \eta(PE + C^{\top})(PE + C^{\top})^{\top} + (1+\tfrac{1}{\eta})\sigma^2 I\Big)x_i < 0$$

If LMI (13) is satisfied, the matrix term in parentheses is strictly negative definite, which implies:

$$\dot{V} \leq -\chi_i^{\top}\chi_i + \gamma^2\chi_{i-1}^{\top}\chi_{i-1}. \tag{15}$$

Therefore, in the absence of input ($\chi_{i-1} = 0$), V decreases strictly, proving asymptotic stability. Otherwise, by integrating $\dot{V}$, the input–output inequality proves string stability such as (14) with gain γ. This completes the proof. □

Design Procedure

Theorem 1 provides conditions if η and σ are known, but in practice they are unknown, so if we want to construct the triggering law, we must use a different approach.

Corollary 1. The conditions in Theorem 1 are equivalent to

$$S(\eta) := \begin{bmatrix} A^{\top}P + PA + C^{\top}C & PE + C^{\top} & PB \\ (PE + C^{\top})^{\top} & -\frac{1}{\eta}I & 0 \\ (PB)^{\top} & 0 & -\gamma^2 I \end{bmatrix} \prec 0 \tag{16}$$

and

$$\sigma < \sigma^*(\eta) = \sqrt{\frac{-\lambda_{\max}(S(\eta))}{1 + 1/\eta}} \tag{17}$$

with $\lambda_{\max}(S(\eta))$ the highest eigenvalue of $S(\eta)$.

In practice, the following procedure can be used to design an event-triggered control system for a vehicle platoon:

(1) **Choose the parameter η.** In practice, any η can be chosen as long as there exists a symmetric matrix $P \succ 0$ such that LMI (16) in Corollary 1 holds.
(2) **Define the upper bound $\sigma^*(\eta)$.** Maximize the triggering threshold $\sigma^*(\eta)$ of Corollary 1 while keeping the LMI feasible.
(3) **Define the proportional triggering law.** Implement the event-triggering condition (6), restated below for clarity:
$$\|e_{u,i-1}(t)\| \leq \sigma \|x_i(t)\|, \qquad \forall t.$$
Any σ such as $0 < \sigma < \sigma^*(\eta)$ ensures that the sampling error is small enough to ensure the decay of the Lyapunov function and the desired dissipation inequality (14).

Remark 1. The triggering condition is sufficient to guarantee that the residual error terms do not compromise the Lyapunov decrease. A potential concern in event-triggered implementations is the occurrence of Zeno behavior, i.e., infinitely many triggering instants in a finite time interval. In our case, Zeno behavior is excluded under mild assumptions on the dynamics of $x(t)$ and the update law of $\hat{u}(t)$. Indeed, the error $e_{u,i-1}(t) = \hat{u}_{i-1}(t) - u_{i-1}(t)$ is reset to zero at each triggering instant, and subsequently evolves continuously according to the dynamics of $u_{i-1}(t)$ and $\hat{u}_{i-1}(t)$. Therefore, immediately after a reset, $|e_{u,i-1}(t)| = 0$ and the triggering condition is not violated. Since $e_{u,i-1}(t)$ is continuous between transmissions, a nonzero time interval is required before the condition is met again. This precludes Zeno phenomena.

In summary, the proposed triggering mechanism simultaneously guarantees:

- asymptotic stability of each vehicle in the absence of inputs,
- string stability with a prescribed $\mathcal{L}_2$ gain bound γ, and
- implementability of the event-triggered law without Zeno accumulation.

3.2 Stability analysis under constant ETC

Theorem 1 establishes asymptotic stability of the origin under the proportional triggering law. This proportional condition enforces a state-dependent bound on the signal error. However, when $\|x_i\|$ is small, the bound becomes very tight, potentially leading to unnecessarily frequent triggering events. In practice, to alleviate communication constraints and avoid arbitrarily fast triggering near the origin, it is common to relax the condition into a constant bound of the form (7), restated below for clarity:
$$\|e_{u,i-1}(t)\| \leq \varepsilon,$$
with $\varepsilon > 0$ a design parameter.

Next, Theorem 2 provides a practical relaxation of Theorem 1 as a result of replacing the state-dependent bound with a constant one.

Theorem 2. (Practical Stability under constant-threshold predictive ETC). For system (10), assume that there exist $P = P^\top \succ 0$, $\gamma > 0$ and $\eta > 0$ such that LMI (16) holds, i.e., $S(\eta) \prec 0$.

Let $\varepsilon > 0$ denote the constant triggering threshold satisfying $\|e_{u,i-1}(t)\| \leq \varepsilon$ for all t and define
$$\rho := \sqrt{\tfrac{1+1/\eta}{-\lambda_{\max}(S(\eta))}}. \tag{18}$$
Then, the following properties hold:

(1) (**Individual stability**) If $\chi_{i-1} \equiv 0$, the set
$$\mathcal{S}_\rho = \Big\{ x_i \in \mathbb{R}^n : \|x_i\| \leq \rho\varepsilon \Big\},$$
is globally asymptotically stable.
(2) (**String stability**) For nonzero χ_{i-1}, the system is $\mathcal{L}_2$ string stable with gain γ, i.e.
$$\|\chi_i\|_{L_2} \leq \gamma \|\chi_{i-1}\|_{L_2}.$$

Proof: Following the same steps as in the proof of Theorem 1, to have $\dot{V} \leq -\chi_i^\top \chi_i + \gamma^2 \chi_{i-1}^\top \chi_{i-1}$, we must ensure that
$$x_i^\top \Big(A^\top P + PA + C^\top C + \tfrac{1}{\gamma^2} PBB^\top P + \eta(PE + C^\top) \cdot (PE + C^\top)^\top \Big) x_i + (1 + \tfrac{1}{\eta}) e_{u,i-1}^\top e_{u,i-1} < 0.$$

If the LMI (16) is satisfied, the matrix term in parentheses is strictly negative definite and compensates for the positive term induced by the constant triggering condition. One obtains
$$\lambda_{\max}(S(\eta)) x_i^\top x_i + (1 + \tfrac{1}{\eta})\varepsilon^2 < 0.$$
This is true for all $\|x_i\| > \rho\varepsilon$, which guarantees asymptotic convergence of $x_i(t)$ toward $\mathcal{S}_\rho$ when $\chi_{i-1} = 0$ and string stability otherwise. □

The coefficient ρ determined by (18) quantifies the system's sensitivity to communication errors and depends solely on the internal dynamics through $S(\eta)$. As for the parameter ε, it defines the triggering threshold for communication, and therefore determines how accurately the reconstructed signal $\hat{u}_{i-1}(t)$ follows the actual signal $u_{i-1}(t)$.

- **Small ε:** triggers occur more frequently, leading to higher communication rates but better tracking performance and smaller steady-state errors.
- **Large ε:** reduces the number of transmissions and alleviates network load, but increases the approximation error and enlarges the steady-state region around the origin.

As a result, the volume of the set $\mathcal{S}_\rho$ captures the trade-off between communication efficiency and control performance. For a given threshold ε, a smaller ρ yields a tighter invariant set and thus better tracking accuracy.

The control design objective is therefore twofold:

(1) Choose ε as small as possible to ensure good performance while keeping the communication rate within acceptable limits.
(2) Minimize ρ over $\eta > 0$ and $S(\eta) \prec 0$ to reduce the size of $\mathcal{S}_\rho$ and enhance robustness to communication imperfections.

4. CONSTRUCTION OF THE PREDICTED INPUT

Here, we take the perspective of the vehicle sending the profile, to which we refer by index i for the remainder. The function f_i introduced in (8) defines the evolution of the predicted control signal $\hat{u}_i(t)$ between two transmission instants of the vehicle. Its construction determines how well the next vehicle $i+1$ can approximate control input $u_i(t)$ in the absence of communication. Although the stability guarantees established in Section 3 hold for any bounded choice of f_i, its design strongly influences the communication rate and transient performance. Under nominal operation, $e_{u,i}(t) \approx 0$, and communication remains silent. When a deviation occurs (e.g., emergency braking due to a pedestrian crossing), the mismatch increases until the trigger rule is violated, which triggers a new prediction to transmit. A more accurate prediction delays the triggering condition and thus reduces the number of transmissions, while a poor prediction accelerates it, potentially leading to a communication cascade along the platoon.

4.1 From Classical Hold Strategies to Predictive Profiles

In the literature, two main hold strategies are commonly used for event-triggered or sampled-data systems:

- **Zero-Order Hold (ZOH):** the transmitted control value is kept constant between updates, i.e., $\dot{\hat{u}}_i(t) = 0$. This approach performs well in steady-state conditions but poorly during transients, since no information about the input evolution is preserved.
- **First-Order Hold (FOH):** the derivative at the transmission instant t_k is also transmitted, resulting in a linear evolution $\dot{\hat{u}}_i(t) = \dot{u}_i(t_k)$. This method improves transient tracking but still neglects the nonlinear behavior of the vehicle over time.

Both methods can be viewed as particular cases of (8) with specific forms of $f_i(t-t_k)$. They are simple to implement but limited in their ability to capture realistic control variations or disturbances.

4.2 Model-based Predictive Construction

In the proposed predictive event-triggered framework, the evolution of $\hat{u}_i(t)$ between two transmission instants is not assumed constant or linear, but rather derived from the internal dynamics of the vehicle. To this end, vehicle i uses its own model and control law to simulate its nominal behavior over a future time window. As long as the real trajectory of $u_i(t)$ follows its nominal model, no further communication is required, and the next vehicle $i+1$ can simply keep using the transmitted prediction of $u_i(t)$.

Nominal closed-loop dynamics. Under ideal conditions where $e_{u,i}(t) = 0$, the internal dynamic of vehicle i is governed by the same differential equations as in (3) but with the difference that vehicle i uses the profile $\hat{u}_{i-1}$ received from its previous vehicle $i-1$ instead of the actual input u_{i-1}. We can consequently define an internal substate $\hat{x}_i = (v_{i-1} - v_i, a_{i-1}, e_i, a_i, u_i)^\top$ local to each vehicle and subject to the system

$$\begin{cases} \dot{\hat{x}}_i(t) = \hat{A}\hat{x}_i(t) + \hat{B}\hat{u}_{i-1}(t), \\ \hat{u}_i(t) = u_i(t) = [0\ 0\ 0\ 0\ 1]\,\hat{x}_i(t), \end{cases} \tag{19}$$

where

$$\hat{A} = \begin{bmatrix} 0 & 1 & 0 & -1 & 0 \\ 0 & -\frac{1}{\tau} & 0 & 0 & 0 \\ 1 & 0 & 0 & -h & 0 \\ 0 & 0 & 0 & -\frac{1}{\tau} & \frac{1}{\tau} \\ \frac{k_d}{h} & 0 & \frac{k_p}{h} & -k_d & -\frac{1}{h} \end{bmatrix}, \quad \hat{B} = \begin{bmatrix} 0 & \frac{1}{\tau} & 0 & 0 & \frac{1}{h} \end{bmatrix}^\top.$$

This nominal system captures the deterministic evolution of vehicle i in the absence of communication errors or disturbances. It used to predict the future control signal $\hat{u}_i$ to be passed on to the next vehicle $i+1$.

Computation of the predictive profile. At each transmission instant t_k, vehicle i integrates (19) forward in time using the current state $\hat{x}_i(t_k)$ and the last received profile $\hat{u}_{i-1}(t)$ from its own predecessor:

$$\hat{x}_i(t) = e^{\hat{A}(t-t_k)}\hat{x}_i(t_k) + \int_{t_k}^{t} e^{\hat{A}(t-\tau)}\hat{B}\,\hat{u}_{i-1}(\tau)\,d\tau, \tag{20}$$

$t \in [t_k, t_k + T_p]$, where T_p denotes the prediction horizon. The first term represents free evolution of the vehicle's internal state, and the second term accounts for the influence of the last received profile $\hat{u}_{i-1}(t)$. From this trajectory, the control output is recovered as

$$\hat{u}_i(t) = [0\ 0\ 0\ 0\ 1]\,\hat{x}_i(t).$$

Transmission of the predicted input. The temporal evolution of $\hat{u}_i(t)$ defines the prediction function f_i in (8). By differentiating the expression above, one obtains

$$\begin{aligned} f_i(t-t_k) = \dot{\hat{u}}_i(t) &= [0\ 0\ 0\ 0\ 1]\,\dot{\hat{x}}_i(t) \\ &= [0\ 0\ 0\ 0\ 1]\left(\hat{A}\hat{x}_i(t) + \hat{B}\hat{u}_{i-1}(t)\right). \end{aligned} \tag{21}$$

Hence, f_i encodes the instantaneous rate of change of the predicted input according to the nominal vehicle dynamics. In principle, transmitting f_i as a continuous function to the next vehicle would allow perfect reconstruction of the control evolution. However, in practical V2V networks, such continuous communication is infeasible. The transmission medium is governed by the IEEE 802.11p standard for dedicated short-range communications, which enables low-latency exchanges in the 5.9 GHz band but is limited by strict payload and rate constraints.Typical V2V packets carry a few hundred bytes and are broadcast at frequencies of 10–100 Hz.

To meet these practical constraints, our approach can be modified to transmit only a lightweight representation of f_i instead of its full continuous evolution (note that in our simulations below, we do not do this). At each triggering instant t_k, vehicle i samples and encodes f_i over its prediction horizon T_p into a small set of representative values (e.g., curvature indicators or key samples). This compact message typically fits within IEEE 802.11p limits. Upon reception of this packet, the next vehicle $i+1$ can reconstruct an approximate trajectory of $\hat{u}_i(t)$.

4.3 Practical Advantages

Our construction differs fundamentally from classical ZOH or FOH schemes. As shown in Figure 1, instead of maintaining a constant (red) or linearly varying (blue) input,

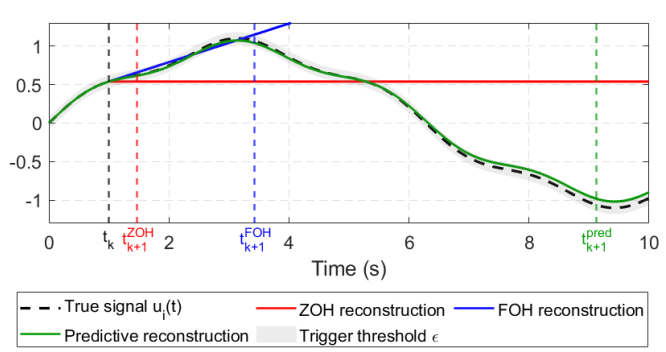

Fig. 1. Comparison of prediction strategies for $\hat{u}_i(t)$. ZOH and FOH strategies typically trigger transmissions much sooner (at times $t_{k+1}^{\text{ZOH}}, t_{k+1}^{\text{FOH}}$ in this example) than the predictive input profile (at time t_{k+1}^{pred}).

the prediction propagates a dynamically consistent trajectory (green). As a result:

- $\hat{u}_i(t)$ preserves the nominal dynamic behavior of the predecessor under normal conditions;
- communication is required only when perturbations (e.g., emergency braking, actuator faults) cause deviations from the predicted profile;
- the derivative f_i naturally remains bounded and smooth, satisfying the stability conditions of Section 3.

4.4 Alternative Prediction Strategies

Although this work focuses on model-based prediction, other formulations of f_i could also be considered within the same framework, such as: 1) polynomial or spline extrapolations fitted on past control data rather than future control data from a nominal model; 2) learning-based predictors using local data to forecast driver or actuator behavior. These alternatives could further enhance prediction quality and robustness under uncertainty, offering promising directions for future research.

5. SIMULATION RESULTS

To validate the proposed prediction-based ETC framework, numerical simulations are performed on a platoon composed of one leader ($i = 0$) and $N = 6$ follower vehicles. Each vehicle follows the dynamics (10) with an actuator time constant $\tau = 0.1$ s. The controller gains $k_p = 2$ and $k_d = 1$ are selected to ensure both individual and string stability under ideal (continuous) communication. The leader follows a reference trajectory that accelerates the platoon from rest to a cruising speed of 120 km/h but which will be subject to two types of disturbance:

- An **instantaneous perturbation**, representing an unexpected obstacle detected by the leader's sensors. This results in a controlled braking maneuver modeled as a smooth velocity bump over the interval $[18, 22]$s. Note that once the obstacle is detected, the previous leader input prediction becomes invalid, but a new predicted signal becomes available, generated e.g. by a model-predictive controller planning a long-horizon reaction to the perturbation. This new prediction can be directly exploited by our framework after in principle a single communication event, unlike in ZOH or FOH methods.
- An **sustained, unknown perturbation**, modeled as $\Delta v_0(t) = 2\sin(t)$ km/h, a low-amplitude sinusoidal disturbance on the leader's velocity, representing driver oscillations or small road-grade variations. In contrast to the instantaneous perturbation above, this signal is never predictable.

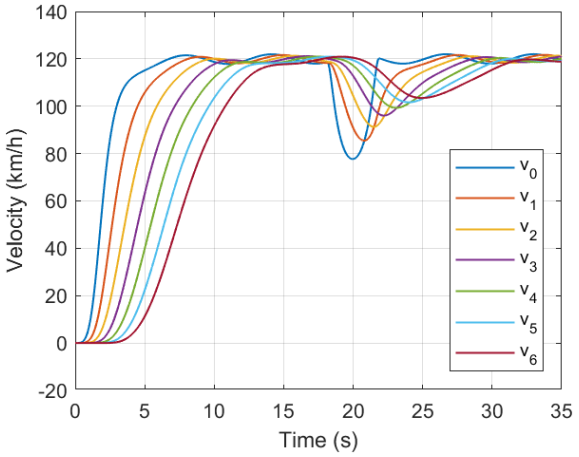

Fig. 2. Velocity trajectories of all vehicles under the predictive ETC.

The event-triggered mechanism is implemented using the constant triggering rule $\|e_{u,i-1}(t)\| \leq \varepsilon$, with $\varepsilon = 0.2$ chosen to guarantee practical stability (see Section 3.2). Minimizing the sensitivity parameter in (18) yields $\rho^* \approx 2.76$ for $\eta^* \approx 4.74$. In steady-state conditions, the trajectories converge asymptotically toward the minimal invariant set

$$\mathcal{S}_\rho = \Big\{ x_i \in \mathbb{R}^n : \|x_i\| \leq 0.55 \Big\},$$

which remains well within the minimum safety margin r between vehicles, thus preserving safe inter-vehicle distances. The predictive profile is computed using a horizon $T_p = 1$ s, after which the function f_i is extrapolated to maintain a smooth prediction.

Figure 2 displays the velocity profiles of all seven vehicles. The platoon accelerates smoothly to 120 km/h before the perturbation. When the braking of the leader occurs, the disturbance propagates downstream with clear attenuation—demonstrating that the predictive ETC preserves both individual stability and string stability. The small oscillations induced by the sinusoidal disturbance remain bounded and do not amplify along the platoon.

The leader's control input u_0 and its predicted version $\hat{u}_0$ are shown in Figure 3. The inset highlights that communication events occur whenever the prediction error $e_{u,0} = u_0 - \hat{u}_0$ exceeds $\varepsilon = 0.2$. As observed, $\hat{u}_0$ follows u_0 throughout most of the trajectory. The known disturbance is well anticipated by follower, and communication events occur mainly when unknown disturbances cause model–signal deviation (or when the prediction horizon T_p is exceeded).

Table 1 summarizes the number of communication received by each vehicle. Compared to the ZOH approach, the predictive strategy significantly reduces the number of transmissions—by nearly an order of magnitude for all vehicles. For instance, vehicle 1 received only 62 times

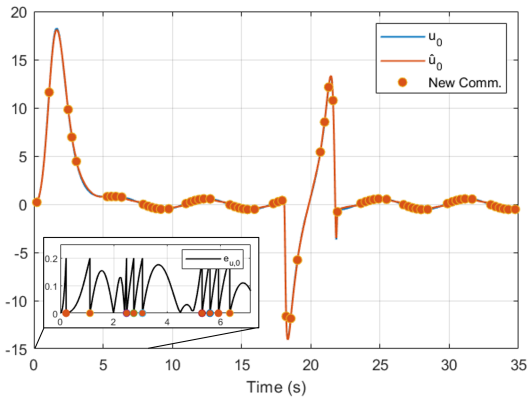

Fig. 3. Comparison between u_0 and $\hat{u}_0$ under the predictive ETC.

instead of 514, while the sixth follower received 24 instead of 91 messages.

Table 1. Number of communication received per vehicle.

Vehicle	ZOH	Prediction-based
1	514	62
2	258	47
3	169	38
4	127	30
5	107	25
6	91	24

6. CONCLUSION

This paper presented a predictive event-triggered communication scheme for vehicle platoons, where each follower anticipates its predecessor's control input using a model-based prediction. Unlike conventional Zero- or First-Order Hold-based methods, this approach maintains individual and string stability while drastically reducing communication needs, since transmissions occur only when real perturbations deviate from the predicted nominal dynamics. Numerical simulations with a seven-vehicle platoon illustrate practical stability and show a significant reduction in communication events without degrading performance. Future work will address adaptive tuning of the prediction horizon and robustness to delays and model uncertainties.

REFERENCES

Chuang, P., Liu, Y., and Gao, H. (2013). Autonomous platoon controller design: A frequency-domain approach. In *2013 9th International Conference on Information, Communications & Signal Processing*, 1–5.

Dang, F., Chen, D., Chen, J., and Li, Z. (2024). Event-triggered model predictive control with deep reinforcement learning for autonomous driving. *IEEE Transactions on Intelligent Vehicles*, 9(1), 459–468.

Dolk, V.S., Ploeg, J., and Heemels, W.M.H. (2017). Event-triggered control for string-stable vehicle platooning. *IEEE Transactions on Intelligent Transportation Systems*, 18(12), 3486–3500.

Feng, S., Zhang, Y., Li, S.E., Cao, Z., Liu, H.X., and Li, L. (2019). String stability for vehicular platoon control: Definitions and analysis methods. *Annual Reviews in Control*, 47, 81–97.

Giambene, G., Rahman, M.S., and Vinel, A. (2020). Analysis of V2V Sidelink Communications for Platoon Applications. In *ICC 2020 - 2020 IEEE International Conference on Communications (ICC)*, 1–6. ISSN: 1938-1883.

He, N., Shi, D., and Chen, T. (2018). Self-triggered model predictive control for networked control systems based on first-order hold. *International Journal of Robust and Nonlinear Control*, 28(4), 1303–1318.

Jang, Y.H. and Kim, H.S. (2024). Sampled-Data Cooperative Adaptive Cruise Control for String-Stable Vehicle Platooning with Communication Delays: A Linear Matrix Inequality Approach. *Machines*, 12(3), 165.

Nardini, G., Virdis, A., Campolo, C., Molinaro, A., and Stea, G. (2018). Cellular-V2X Communications for Platooning: Design and Evaluation. *Sensors*, 18(5), 1527.

Ploeg, J., Shukla, D.P., van de Wouw, N., and Nijmeijer, H. (2014). Controller Synthesis for String Stability of Vehicle Platoons. *IEEE Transactions on Intelligent Transportation Systems*, 15(2), 854–865.

Ploeg, J., Van De Wouw, N., and Nijmeijer, H. (2013). Lp string stability of cascaded systems: Application to vehicle platooning. *IEEE Transactions on Control Systems Technology*, 22(2), 786–793.

Razzaghpour, M., Valiente, R., Zaman, M., and Fallah, Y.P. (2023). Predictive Model-Based and Control-Aware Communication Strategies for Cooperative Adaptive Cruise Control. *IEEE Open Journal of Intelligent Transportation Systems*, 4, 232–243.

Shladover, S.E. (2018). Connected and automated vehicle systems: Introduction and overview. *Journal of Intelligent Transportation Systems*, 22(3), 190–200.

Swaroop, H. (1997). String stability of interconnected systems: An application to platooning in automated highway systems. *Transportation Research Part A: Policy and Practice*, 31(1), 65.

Tabuada, P. (2007). Event-triggered real-time scheduling of stabilizing control tasks. *IEEE Transactions on Automatic Control*, 52(9), 1680–1685.

Toker, O., Shah, A., and Tureli, M.U. (2018). The ieee 802.11 p performance for different packet length and arrival rate in vanets. In *The 14th Advanced International Conference on Telecommunications*.

Trabelsi, N., Chaari Fourati, L., and Jaafar, W. (2024). Deep reinforcement learning for autonomous SideLink radio resource management in platoon-based C-V2X networks: An overview. *Computer Networks*, 255, 110901.

Varutti, P., Kern, B., Faulwasser, T., and Findeisen, R. (2009). Event-based model predictive control for networked control systems. In *Proceedings of the 48h IEEE Conference on Decision and Control (CDC) held jointly with 2009 28th Chinese Control Conference*, 567–572.

Wang, B. and Gu, G. (2025). A Passivity Approach to String Stability and Distributed Adaptive Control of Vehicle Platoons. *IEEE Transactions on Vehicular Technology*, 74(8), 11698–11714.